Journal of Medicinal Chemistry

Article

pubs.acs.org/jmc

A Selective Mitochondrial-Targeted Chlorambucil with Remarkable Cytotoxicity in Breast and Pancreatic Cancers

Melissa Millard,[†] John D. Gallagher,[†] Bogdan Z. Olenyuk,*[,†] and Nouri Neamati*[,†,‡]

[†]Department of Pharmacology and Pharmaceutical Sciences, School of Pharmacy, University of Southern California, 1985 Zonal Avenue, Los Angeles, California 90089, United States

[‡]Department of Medicinal Chemistry, College of Pharmacy, and Translational Oncology Program, University of Michigan, 2800 Plymouth Road, Building 520, Room 1363, Ann Arbor, Michigan 48109, United States

Supporting Information

ABSTRACT: Nitrogen mustards, widely used as chemotherapeutics, have limited safety and efficacy. Mitochondria lack a functional nucleotide excision repair mechanism to repair DNA adducts and are sensitive to alkylating agents. Importantly, cancer cells have higher intrinsic mitochondrial membrane potential ($\Delta\psi_{mt}$) than normal cells. Therefore, selectively targeting nitrogen mustards to cancer cell mitochondria based on $\Delta\psi_{mt}$ could overcome those limitations. Herein, we describe the design, synthesis, and evaluation of Mito-Chlor, a triphenylphosphonium derivative of the nitrogen mustard chlorambucil. We show that Mito-Chlor localizes to cancer cell mitochondria where it acts on mtDNA to arrest cell cycle and induce cell death, resulting in a 80-fold enhancement of cell kill in a panel of breast and pancreatic cancer cell lines that are insensitive to the parent drug. Significantly, Mito-Chlor delayed tumor progression in a mouse xenograft model of human pancreatic cancer. This is a first example of repurposing chlorambucil, a drug not used in breast and pancreatic cancer treatment, as a novel drug candidate for these diseases.

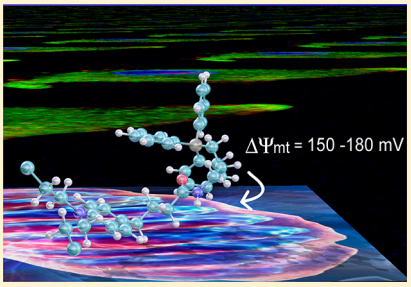

INTRODUCTION

Chlorambucil (**1**, Chart 1), a member of the nitrogen mustard class of DNA alkylating agents, is used primarily for the treatment of chronic lymphocytic leukemia (CLL), lymphomas such as Hodgkin's Disease and non-Hodgkin lymphoma, Waldenström's macroglobulinemia, and some solid tumors.[1] The nitrogen mustards share a common mechanism of action stemming from the presence of an *N*,*N*-bis(2-chloroethyl)-amine group. This moiety readily reacts with intracellular components such as proteins, phospholipids, and nucleic acids; covalent modification of proteins and phospholipids can have modest inhibition of cellular function, while alkylation of genomic DNA is the primary mechanism of cytotoxicity. Chlorambucil modifies DNA through the formation of either mono- or bifunctional adducts.[2] Monoadducts interfere with gene expression and promote mismatched base-pairing, while bifunctional alkylation creates intra- and interstrand cross-links that inhibit DNA synthesis and cause double-strand breaks.[3,4] In this way, exposure to chlorambucil leads to apoptotic cell death via the accumulation of persistent DNA damage.[5]

Issues of drug stability, selectivity, and resistance are common to this class of alkylating agents. The high spurious reactivity and short half-life of nitrogen mustards can attenuate their potency. Covalent interactions with proteins and phospholipids can sequester drug from the site of action such that <10% of the original dose may be available to interact with DNA. These consequences of instability and reactivity are compounded by the slow rate of passive drug uptake. In the end, overcoming "off-target" binding and drug instability requires higher dosages to produce a therapeutic response.

The lack of selectivity for tumor cells is another concern. In the short term, myelosuppression, the primary dose-limiting toxicity, increases the risk of serious infections. Over the longer term, cumulative damage to normal tissues significantly increases the probability of developing secondary neoplasms.[1] In addition to toxicity, repeated administration eventually leads to drug resistance for most patients.[6] In a recent analysis of several phase III clinical trials, dose and duration of treatment were identified as two important determinants of response to chlorambucil.[7] Thus, the toxicity and drug resistance associated with nitrogen mustards are serious impediments of therapeutic efficacy. Conversely, enhancement of chlorambucil tissue selectivity, drug accumulation, and tumor sensitivity could significantly benefit treatment outcomes.

Chlorambucil was one of the first DNA damaging agents used for chemotherapy and for decades was considered the standard of care for CLL because it produced the lowest dose-limiting toxicity in its class. Although newer drugs have taken the place of chlorambucil in current CLL chemotherapeutic regimens, the fact that it remains a first-line treatment for CLL in the elderly and immune-suppressed patients underscores its continued relevance as an anticancer agent.[7,8] Certain advanced cancers, such as hormone refractory or hormone receptor negative breast cancers and pancreatic adenocarcinomas often

Received: August 12, 2013
Published: October 22, 2013

Chart 1. Structures of Chlorambucil (1) and Design of Conjugates Mito-Chlor (2), Tributyl-Mito-Chlor (3), Tricyclohexyl-Mito-Chlor (4), and Dihydroxy-Mito-Chlor (5)

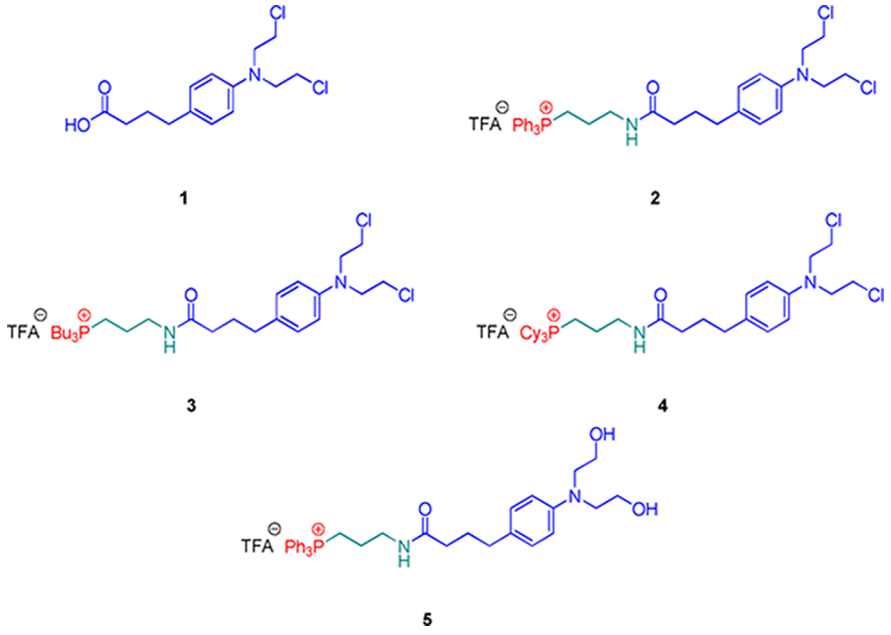

Scheme 1. Synthesis of Mito-Chlor Related Conjugates and Control 5[a]

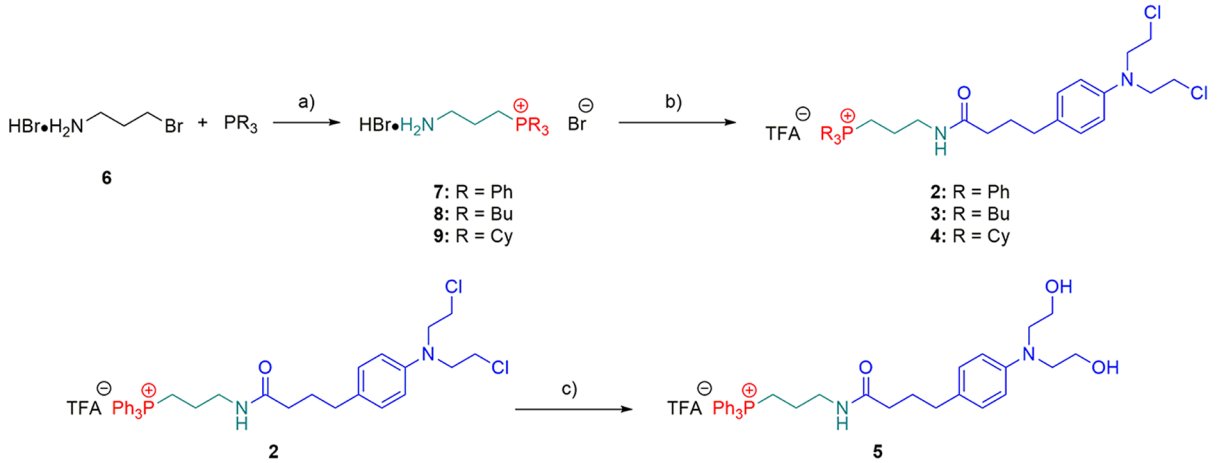

[a](a) MeCN, reflux; (b) chlorambucil, DIPEA, HBtU, DCM; (c) acetonitrile, H_2O, 90 °C.

fail to respond to current regimens. The repurposing of "tried and true" agents such as chlorambucil may enhance treatment for these patients. Thus from a medicinal chemistry standpoint, tissue selectivity and drug resistance are foci that could expedite the repurposing of chlorambucil.

The well documented differences in mitochondrial membrane potential ($\Delta\psi_{mt}$) between normal and cancer cells[9] make mitochondria an attractive target in the design of next-generation anticancer therapeutics. In keeping with these considerations, we hypothesized that directing chlorambucil to cancer cell mitochondria might be an effective approach to combat issues of safety and drug resistance. Linkage to a lipophilic cation to exploit the higher mitochondrial membrane potentials of solid tumors, we reasoned, would improve tissue selectivity and hasten drug uptake. Additionally, the lack of a nucleotide excision repair mechanism (NER) in mitochondria might sensitize otherwise resistant cells to the DNA damaging effects of nitrogen mustards.[10,11]

To this end, we designed and synthesized a series of mitochondria-targeted phosphonium salt derivatives of chlorambucil **2**–**5** (Chart 1). When screened in a panel of human carcinoma cell lines, derivative **2**, which we named Mito-Chlor, exhibited remarkable potency compared to the parent drug. The sensitivity of cell lines resistant to chlorambucil was dependent on the ability of Mito-Chlor to enter mitochondria and bind mtDNA. Once in the mitochondria, Mito-Chlor caused S-phase specific cell cycle arrest consistent with mtDNA damage and acted to increase nuclear histone H2A.X phosphorylation (γH2A.X). Interestingly, Mito-Chlor induced DNA double-strand breaks manifested by the elevated levels of γH2A.X, but not Mito-Chlor cytotoxicity, was reversible upon treatment with *N*-acetyl cysteine.

RESULTS

A Two-Step Synthetic Method for Preparation of Mito-Chlor. Using the carboxylic acid functional group as a

dx.doi.org/10.1021/jm4012438 | J. Med. Chem. 2013, 56, 9170–9179

point of attachment, we designed a facile, two-step method of phosphine conjugation suitable for large-scale production of conjugates. Synthesis of Mito-Chlor, (3-(4-(4-(bis(2-chloroethyl)amino)phenyl)butanamido)propyl) triphenylphosphonium trifluoroacetate (**2**), was carried out as illustrated in Scheme 1. Initially, 3-bromopropylamine hydrobromide (**6**) was reacted with triphenylphosphine in refluxing acetonitrile for 16 h. The resulting intermediate (**7**) was readily isolated and required only crystallization from diethyl ether−2-propanol to obtain pure material. The final product **2** was prepared starting with chlorambucil **1** via a standard coupling protocol using DMAP, **7**, *N*,*N*-diisopropylethylamine, and then HBtU. Tributyl- and tricyclohexylphosphonium chlorambucil conjugates **3** and **4** were synthesized analogously using 3-aminopropyltributylphosphonium bromide **8** and 3-aminopropyltricyclohexylphosphonium **9**, respectively. Finally, the negative control, TPP-dihydroxychlorambucil **5**, was prepared by hydrolyzing **2** in acetonitrile/water at 80 °C. Compound **5** is not able to produce aziridinium ion in a manner similar to **2** (vide infra), and it was included in the assays in order to rule out the potential off-target effects of **2** in vitro that could be caused by other than DNA alkylation mechanisms.

Phosphonium Salt Derivatives of Chlorambucil Have Antiproliferative Activity. The newly synthesized phosphonium salt derivatives and the parent drug (**1**) were screened for antiproliferative activity in the MCF7 breast cancer cell line using the colorimetric MTT assay (see Experimental Section). To determine the concentration of compound that could inhibit cell viability and/or proliferation by 50% (IC_{50} concentration), cells were treated for 72 h with increasing amounts of **1**−**5**, ranging over three to four logs of concentrations. The results of this screening, shown in Table 1, provide a simple structure−activity relationship (SAR) for

Table 1. IC_{50} Values of 1−5 in MCF7 Cell Line

IC_{50} (μM)				
chlorambucil (**1**)	**2**	**3**	**4**	**5**
100 ± 2.3	7.0 ± 1.2	35.0 ± 3.8	40.0 ± 5.1	80.0 ± 3.9

these conjugates. The parent drug had weak activity in the MCF7 cell line, having an IC_{50} concentration of 100 μM. Modification of **1** through the introduction of lipophilic phosphonium salts, as in compounds **2**−**4**, enhanced the activity of chlorambucil. Of the three phosphonium derivatives, triphenylphosphonium **2** had the lowest IC_{50}, suggesting that the presence of aryl rings provide greater potency than do saturated hydrocarbons. In contrast, negative control TPP-dihydroxychlorambucil **5** has shown >10-fold reduced potency as compared to **2**, suggesting that DNA alkylation still remains one of the main mechanisms of enhanced cytotoxicity of **2**.

Conjugation to Triphenylphosphonium Cation Reverses Chlorambucil Resistance. To expand on the results obtained in the MCF7 cell lines, we screened **1** and **2** in a panel of breast cancer cell lines of different origin. The cell lines comprising this panel were representative of typical molecular subtypes encountered in clinical practice and varied considerably in hormone receptor and HER2/neu status (Supporting Information Table S1). The resulting IC_{50} values for **1** and **2** in each cell line are presented in Table 2 along with the sensitivity ratio. The sensitivity ratio represents the fold change in IC_{50} value between the parent drug **1** and Mito-Chlor **2**. None of the cell lines were sensitive to chlorambucil at concentrations below 20 μM, with their IC_{50} concentrations ranging from 44 μM to over 500 μM. In contrast, the entire panel of cell lines was highly sensitive to Mito-Chlor. For each of the cell lines tested, the IC_{50} concentration of **2** was significantly lower than that of **1**, all ranging from 1.7 to 11.4 μM. Interestingly, MBA-MB-468 was most sensitive to Mito-Chlor, having the lowest IC_{50} (1.7 μM), whereas CAMA-1 with a sensitivity ratio of 79.9 has shown the greatest increase in potency in response to **2** (Table 2).

Further antiproliferative screening was carried out in a small panel of pancreatic cancer cell lines (Supporting Information Table S2). A similar increase in potency was observed in two pancreatic cancer cell lines treated with **2** (Table 3). The IC_{50} values for MIA PaCa-2 and BxPC-3 treated with **2** were 1.6 and 2.5 μM, respectively. Each of these values represents a remarkable (>40-fold) increase in potency over the parent drug **1**. Overall, these results demonstrate a significant increase in potency of **2** as a result of conjugation to the triphenylphosphonium cation.

Table 3. IC_{50} Values of 1 and 2 in a Panel of Pancreatic Ductal Adenocarcinoma Cell Lines

	MIA PaCa-2	BxPC3
1	78.3 ± 0.3	>100
2	1.6 ± 0.9	2.5 ± 2.8
sensitivity ratio	48.9	>40

Mito-Chlor Localizes to Mitochondria. To determine if this increase in potency was due to mitochondrial targeting, the subcellular localization of **2** was examined by laser-scanning confocal microscopy (Figure 1). MIA PaCa-2 cells treated with

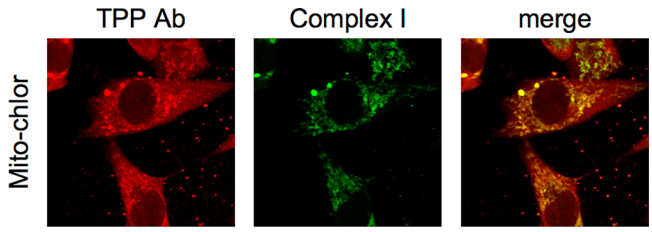

Figure 1. Confocal images of MIA-PaCa-2 treated with 10 μM of Mito-Chlor for 18 h and stained with anti-complex I antibody and anti-TPP antisera.

Table 2. IC_{50} Values for 1 and 2 in a Panel of Breast Cancer Cell Lines

	MDA- MB-435	MCF-7	MDA- MB- 231	MDA- MB-468	CAMA-1	HS578T	SKBR-3	BT549	BT-474
1	150 ± 5.0	73.3 ± 14.4	521.3 ± 249.9	43.8 ± 8.1	191.7 ± 62.9	162.5 ± 88.4	247.5 ± 3.5	>200	237.5 ± 17.7
2	3.0 ± 1.9	9.5 ± 5.7	9.5 ± 5.7	1.7 ± 0.6	2.4 ± 3.0	11.4 ± 4.3	5.7 ± 5.9	7.3 ± 2.9	6.5 ± 3.6
sensitivity ratio	50.0	7.7	54.8	25.8	79.9	14.3	43.4	27.4	36.5

dx.doi.org/10.1021/jm4012438 | J. Med. Chem. 2013, 56, 9170−9179

2 were fixed and costained with antisera specific for the TPP moiety and an antibody raised against complex I of the electron transport chain in combination with fluorescently labeled secondary antibodies. The mitochondrial membrane potential-dependent nature of TPP accumulation dictates that upon loss of mitochondrial integrity, any unbound compound will diffuse out of the mitochondria. Therefore, if **2** enters mitochondria and alkylates mtDNA, the compound should be retained in mitochondria during the fixation and permeabilization process and be readily detectable upon immunofluorescent staining with TPP antisera. Consistent with mitochondrial uptake and mtDNA alkylation, TPP-associated antisera fluorescence showed a distinctive staining pattern similar to that observed for complex I that is known to reside within mitochondria. Cytoplasmic portions of the cell stained diffusely for TPP, whereas the nuclear compartment was devoid of any antisera fluorescence. These results demonstrate localization and retention of Mito-Chlor that is consistent with a mechanism of action that includes mitochondrial uptake and mtDNA alkylation. Positive staining with the TPP antibody also indicates that **2** does not undergo significant β-oxidation within mitochondria but rather interacts with its target as an intact conjugate.

Mito-Chlor Activity Is Dependent on the Presence of Mitochondrial DNA. Building upon these results, we sought to determine whether covalent modification of mtDNA was a necessary step in the mechanism of action of **2**. To this end, we utilized a MDA-MB-231 Rho θ cell line, comparing its sensitivity to **1** and **2** with that of the MDA-MB-231 Rho wild-type cells from which they were derived. Despite being devoid of mtDNA, Rho θ cells maintain mitochondrial membrane potential similar to that of their parental counterpart (Supporting Information Figure S1), making them a suitable model in which to investigate the Mito-Chlor mechanism of action. Having equivalent mitochondrial membrane potential, we can expect similar levels of exposure to treatments in these isogenic cell lines, therefore any difference in sensitivity observed in MDA-MB-231 Rho θ could likely be due to the inability of **2** to interact with mtDNA. With this in mind, an MTT-based cell viability assay was carried out in the MDA-MB-231 Rho θ cell line as described previously for breast and pancreatic cancer cell lines. A comparison of the cellular response to treatment with **1** shows that sensitivities between both cell lines was similar. However, when MDA-MB-231 Rho θ were treated with **2**, there was a clear increase in the IC_{50} concentration, as compared to IC_{50} obtained for the MDA-MB-231 Rho wild-type parent cell line (Table 4). An even more striking difference in sensitivity was found in MDA-MB-435 Rho θ as compared to MDA-MB-435 Rho wild-type cells: when two sublines of MDA-MB-231 Rho θ, W01, and W02 were treated with **2**, the increase in IC_{50} was 5-fold and 11.7-fold, respectively. These results suggest that mtDNA alkylation is at least in part responsible for the mechanism of action of **2**.

Table 4. IC_{50} Values of 1 and 2 in a Panel of Rho θ and Paired Rho Wild-Type Cell Lines

	MDA-MB-435 Rho wt	MDA-435 Rho θ -W01	MDA-435 Rho θ -W02	MDA-MB-231 Rho wt	MDA-231 Rho θ -W02
1	150 ± 5.0	>200	>200	>200	>200
2	3.0 ± 1.9	15.0 ± 4.3	35.0 ± 8.6	9.5 ± 5.7	>20
2 wt: θ ratio		5.0	11.7		>2.1

Mito-Chlor Causes Cell Cycle Arrest Consistent with mtDNA Damage. To further understand the mechanism of action of Mito-Chlor, we compared cell cycle progression in response to **1** and **2**. MIA PaCa-2 cells were treated with each compound at their respective IC_{50} concentrations for 24, 48, and 72 h, and DNA content was analyzed by flow cytometry. The results are shown in Figure 2. At 24 h post-treatment, cells

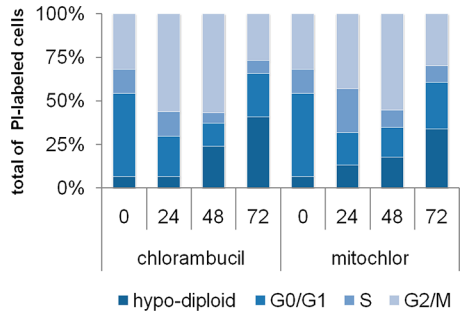

Figure 2. Cell cycle distribution of MIA PaCa-2 at various time points (0−72 h) following treatment with 20 μM of **1** or 2 μM of **2** as determined by flow cytometry.

treated with **1** arrested at the G2/M phase, whereas treatment with **2** increased the number of cells in S-phase accompanied by a secondary block in G2/M progression. By 48 h, the cell cycle distribution was similar for both treatments, most notably the marked arrest in G2/M phase. The percentage of hypodiploid cells increased throughout the duration of treatment, and by 72 h accounted for the highest fraction of stained cells in both treatment groups, resulting from loss of cells in G2/M.

Although chlorambucil is not considered a schedule-dependent drug, as a DNA alkylator it does activate the DNA damage checkpoint causing arrest of cells in the G2 phase of the cell cycle.[12] Damage to mtDNA via oxidative stress or adduct formation results in S-phase arrest accompanied by a moderate G2/M blockade, and disruption of mitochondrial membrane potential with carbonyl cyanide 3-chlorophenylhydrazone (CCCP), a proton ionophore that destroys the membrane potential across the mitochondrial membrane, has been shown to cause G2/M arrest.[13,14]

The cell cycle perturbations induced by **2** at 24 h are consistent with previous reports on the role of mtDNA damage in cell cycle arrest, lending additional support to our hypothesis that mtDNA damage is central to the mechanism of action of **2**. The primarily G2/M arrest noted at 48 h is consistent with the loss of mitochondrial membrane potential that is known to precede mitochondrial-mediated apoptosis.

Mito-Chlor Induced nDNA Damage Is Reversible upon ROS Scavenging. We examined γH2A.X expression as a marker of nuclear DNA (nDNA) damage, expecting that treatment with **1**, but not **2**, would cause an increase in γH2A.X. Histone H2A.X is rapidly phosphorylated at serine 139 (γH2A.X) following the induction of double-strand breaks, while the lack of histones in mtDNA allows discrimination of the subcellular location of DNA damage.[15] We performed Western blot for γH2A.X expression in MIA PaCa-2 and MDA-MB-468 cell lines at various time points following treatment with **1** and **2**. Contrary to our expectations, both treatments caused a time dependent increase in γH2A.X (Supporting Information Figure S2A,B) in each cell line. Modest increases

dx.doi.org/10.1021/jm4012438 | J. Med. Chem. 2013, 56, 9170−9179

were seen at early time points (t < 5 h), with more significant increase occurring later at 5, 8, and 24 h treatment. Mitochondria are a major source of free radicals within the cell. Dysfunctional mitochondria produce higher levels of reactive oxygen species (ROS) than their normal counterparts. Oxidative stress can be linked to genomic instability via ROS induced damage to nDNA in the form of single- and double-strand breaks that when inadequately repaired are capable of triggering apoptosis. For this reason, we sought to investigate whether DNA damage induced by **2** at the level of mitochondria could produce ROS damage to nDNA and if the resulting nDNA damage was involved in or required for cell death. To determine if ROS were responsible for the increase in γH2A.X, we treated cells with **1** and **2** in the presence of the antioxidant *N*-acetyl-cysteine (NAC) for 24 h. Results obtained by Western blot showed a 2.5- and 2.9-fold increase in H2A.X following **1** and **2**, respectively, but only in cells treated with **2** were the phosphorylation levels returned to baseline by the addition of NAC (Figure 3). Despite the ability to reverse signs

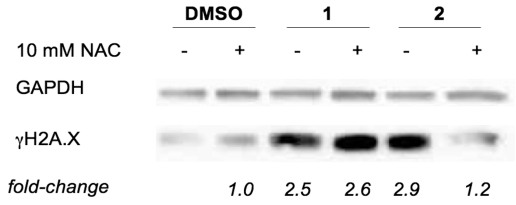

Figure 3. Western blot of MIA-PaCa-2 cells treated with **1** and **2** for 24 h in the presence and absence of *N*-acetyl cysteine. Values represent fold change in γH2A.X expression normalized to GAPDH as calculated by densitometry.

of nDNA damage, NAC treatment did not prevent cell death induced by **2** (Table 5). These results indicate that **2** is still capable of inducing nDNA damage, however Mito-Chlor's mechanism of cell death is distinct from the parent drug.

Table 5. Effect of ROS Scavenging on IC_{50} Values (μM) of 1 and 2 in MDA MB 468 Cell Line[a]

	1	2
− NAC	50 ± 8.1	1.9 ± 0.9
+ NAC	67.5 ± 3.5	0.6 ± 0.3

[a]Where indicated with ± standard deviation, IC_{50} values represent the average of three experiments, performed in triplicate.

Mito-Chlor Suppresses Tumor Growth in a Murine Xenograft of Human Pancreatic Cancer. The in vivo efficacy of Mito-Chlor and chlorambucil was evaluated in a mouse xenograft model of human pancreatic cancer. To this end, established MIA PaCa-2 xenografts were treated 5 times weekly with Mito-Chlor, chlorambucil, or vehicle alone. The mean tumor volume for each group was plotted against the number of days on treatment to give representative growth curves for each treatment group. The results obtained following 36 days treatment are presented in Figure 4. Mito-Chlor caused significant delay in tumor growth when compared to mice receiving vehicle (p = 0.018, t-test). Overall, this represented a 61.5% reduction in tumor size. The parent drug also showed some efficacy, having caused a reduction in average tumor volume close to 45%, however these results did not meet the criteria to be considered statistically significant (p = 0.214, t-test). As a single agent, however, Mito-Chlor was more effective

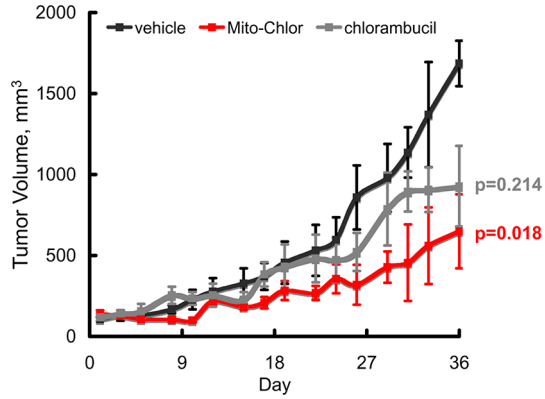

Figure 4. Mito-Chlor inhibits growth of pancreatic cancer xenografts when injected as single agent. Athymic nude mice bearing MIA PaCa-2 xenografts were treated with vehicle (black line), chlorambucil (10 mg/kg, gray line), or Mito-Chlor (10 mg/kg, red line). Points represent mean tumor volume ± SEM. The p values for each treatment group versus vehicle were obtained using student's t test on data obtained at day 36 and are shown to the right of their respective lines.

in delaying tumor growth compared to the parent drug when administered at an equivalent dose.

DISCUSSION

In recent years, intense efforts have focused on improving the therapeutic index of chlorambucil by exploiting tumor specific mechanisms of drug delivery. Generally, these attempts have been successful, often with the added benefits of enhancing drug stability and modest to substantial gains in chlorambucil potency.[16−27] While in vivo drug stability, selectivity, and potency are desirable, the issue of drug resistance remains a key challenge to effective therapy. In an attempt to evade drug resistance through the selection of sensitive populations, there has been a resurgence of interest in chlorambucil for the treatment of certain solid tumors of the breast and pancreas. This renewed attention follows studies indicating that tumor cell lines derived from patients harboring germ-line mutations in BRCA1, BRCA2, FANCC, or FANCG gene loci exhibit in vivo hypersensitivity to DNA cross-linking agents due to the defects in the homologous recombination pathway of DNA repair conferred by these mutations.[28,29] However, without some measure of selectivity, this approach to treatment stratification would likely serve to enhance the already high risk of secondary tumors in this DNA repair deficient population. On the basis of these observations, we concluded that a chlorambucil derivative that could both selectively target tumor cells *and* evade common resistance mechanisms would be of greater overall benefit.

Exploiting phenotypic differences is an effective pharmacologic approach to impart selectivity between normal and cancerous tissues. Our efforts to enhance the selectivity and increase the concentration of chlorambucil at the site of action focused on the well documented differences in mitochondrial membrane potential ($\Delta\psi_{mt}$) between normal and cancer cells.[9] Furthermore, within a tumor mass there can be heterogeneity of $\Delta\psi_{mt}$. Tumor cells with higher $\Delta\psi_{mt}$ show a greater propensity for tumor formation, increased motility and invasive behavior, anchorage-independent growth, the ability to survive under low oxygen conditions, and resistance to apoptosis.[30−32] Thus agents such as Mito-Chlor, that accumulate based on

dx.doi.org/10.1021/jm4012438 | J. Med. Chem. 2013, 56, 9170−9179

$\Delta\psi_{mt}$, can offer selectivity in targeting the most malignant cells within a tumor while sparing most of the healthy, normal tissues.

Recent efforts to target chlorambucil to mitochondria demonstrate the importance of lipophilic cationic properties in subcellular targeting. An estradiene-3-one chlorambucil derivative has been shown to enter the mitochondrial matrix where alkylation and inhibition of complex I function augments the genotoxic effects of nuclear DNA damage for a gain in potency.[33,34] Using a mitochondrial penetrating peptide composed of unnatural amino acids, Fonseca et al. have shown enhanced activity in HL-60 leukemia cell lines compared to the parent drug.[35,61] This approach establishes a strong proof-of-concept for mitochondrial targeting of DNA alkylators, but the clinical applicability may be limited by the lack of in vivo knowledge surrounding this type of delivery mechanism.

For our study, as a means to direct chlorambucil to the mitochondria, we chose the triphenylphosphonium cation. The efficacy with which triphenylphosphonium salts (TPP) accumulate selectively within energized mitochondria based on $\Delta\psi_{mt}$ is well-documented.[36−41] TPP are readily concentrated within cells, initially driven by the potential of the plasma membrane, and then are further concentrated within the mitochondria.[40] As a result, uptake of lipophilic cations into mitochondria increases 10-fold for every 61.5 mV of membrane potential at 37 °C, leading to 100−500-fold accumulation[40] and, for multiple charged species, the differences in concentration between this organelle and the interstitial space could be over 1000-fold. The variation in uptake between cell populations of differing $\Delta\psi_{mt}$ has been estimated to be 10−50-fold. Upon equilibration, TPP cations that do not bind to any targets within mitochondria are released into the cytoplasm and interstitial space, forming a concentration gradient. When mitochondria remain energized, the rate of release is slower than the rate of uptake based on the stabilization conferred by $\Delta\psi_{mt}$. Conversely, upon dissipation of $\Delta\psi_{mt}$, any unbound TPP is rapidly released from mitochondria.[9]

The direct translational feasibility of using the TPP targeting moiety is supported by numerous in vivo studies demonstrating the potential of TPP-based compounds as mitochondrial targeted therapeutics. Phase I and II clinical trials of Mito-Q, a mitochondrial targeted antioxidant, validate the in vivo capacity of TPP-based compounds to accumulate within mitochondria and exert therapeutic effects without systemic toxicity.[42−44] TPP-based PET diagnostic imaging probes have confirmed in vivo tumor selectivity.[45−49] Preclinical studies of novel phosphonium salts including those performed in our own laboratory have previously demonstrated in vivo safety and efficacy in animal models of human cancer.[50,51]

In our current study, we found the TPP cation to be an effective means of delivering chlorambucil to cancer cell mitochondria in vitro. Immunohistochemical staining in breast and pancreatic cancer cells lines both demonstrated uptake and long-term retention of intact Mito-Chlor within the mitochondria. These results clearly illustrate the subcellular localization of Mito-Chlor and rule out direct interaction with nDNA in the mechanism of action. Beyond this, our results also suggest that TPP conjugation may inhibit the formation of toxic metabolites. In vivo, the butyric acid side chain of chlorambucil undergoes rapid and extensive β-oxidation to produce phenylacetic acid mustard (PAAM).[52] PAAM shows similar antiproliferative properties in cell culture but has a lower therapeutic index, greater acute toxicity, and greater teratogenicity than that of chlorambucil.[52−54] Positive staining of fixed cells with an antibody specific for the TPP moiety is contingent upon both the presence of TPP cation and formation of covalent adducts. β-Oxidation of Mito-Chlor would liberate the TPP cation, resulting in loss of signal. Given the robust staining observed, it is possible that, unlike chlorambucil, Mito-Chlor is not a substrate for mitochondrial β-oxidation. Thus if Mito-Chlor cannot be metabolized to PAAM, it may have a more favorable therapeutic profile in vivo.

The lack of sensitivity to chlorambucil treatment observed in our panels of cancer cell lines is typical. Moreover, the majority of pancreatic cancers are intrinsically resistant and most advanced breast cancers eventually become refractory to genotoxic agents.[55,56] In both breast and pancreatic cancers, DSB repair mechanisms have been linked with resistance to genotoxic therapies.[57,58] Chlorambucil damages DNA in multiple ways, but the primary mechanism of chlorambucil cytotoxicity involves the formation of N7G:N7G cross-links.[59] The extent and duration of DNA adducts is a direct determinant of chlorambucil potency.[5] Repair of DNA damage of this type is complex, requiring the engagement and coordination of multiple DNA repair mechanisms including nucleotide excision repair (NER), homologous recombination (HR), and nonhomologous end joining (NHEJ).[59] In terms of drug resistance, sensitivity to chlorambucil is tempered by intrinsic DNA repair mechanisms that are often up-regulated in breast and pancreatic cancer tumors.[59,60] The overexpression of key DNA repair factors involved in HR and/or NHEJ enhances the ability to detect and repair DNA cross-links and adducts that attenuates the effect of DNA damage on tumor cell survival. In the case of nitrogen mustards, this is evidenced by the observation that breast and pancreatic tumors competent for relevant DNA repair factors are significantly less sensitive to chlorambucil compared to incompetent cell lines[28,29] and the significant gains in therapeutic efficacy that are achieved when combining chlorambucil with agents that prevent DNA repair such as PARP inhibitors.[28]

Mitochondrial targeting of chlorambucil produced substantial gains in potency in chlorambucil-resistant breast and pancreatic cancer cell lines. This observation is in agreement with the parallel study that also employed a structurally similar compound as well as mitochondria-targeting peptide−chlorambucil conjugate.[61] We found, however, that unlike the reported similar potency in 143B osteosarcoma cells and their Rho θ sublines, the reversal in resistance caused by mitochondrial targeting was dependent, at least partially, on the presence of mtDNA and was evidenced by the decrease of activity in the MDA-MB-231 Rho θ cell line. The marked variation in drug potency between the parent and Mito-Chlor could be attributed to differences in the rate and extent of DNA repair occurring in the respective cell compartments. The integrity of mtDNA does not appear to be as highly guarded as that of the nuclear genome and, therefore, targeting mtDNA may offer a key to overcoming DNA-repair mediated drug resistance. Although subject to the same genetic insults, compared to the nucleus, mitochondria appear limited in their capacity to repair DNA and thus may be more sensitive to the broad spectrum damage caused by bifunctional alkylating agents.[10,11] Mitochondria lack a functional NER mechanism and are unable to repair DNA cross-links; as a result, intra- and interstrand chlorambucil adducts are long-lived within mitochondrial DNA.[11] Cross-links interfere with mtDNA synthesis and transcription, induce DSBs, and cause mtDNA

dx.doi.org/10.1021/jm4012438 | J. Med. Chem. 2013, 56, 9170−9179

degradation, all of which negatively impact mitochondrial function. Persistent mtDNA damage in the form of oxidative base damage and single-strand breaks is also sufficient to cause mitochondrial dysfunction and trigger apoptosis.[58]

Analysis of DNA content revealed distinct differences in cell cycle distribution between Mito-Chlor and the parent drug. Proliferating cells that sustain damage to nuclear DNA generally arrest in the G2-phase of the cell cycle. Activation of the G2-M checkpoint allows for repair of genetic damage prior to entry into mitosis but can also trigger apoptosis in the event that nDNA damage exceeds the cell's repair capability. In agreement with previous reports in CLL cells, chlorambucil-treated MIA PaCa-2 cells showed early arrest and continued accumulation in the G2/M phase of the cell cycle. Loss of cells from G2/M phase was concomitant with an increase in the percentage of hypodiploid cells and was proportional to the observed IC_{50} concentration. Perturbation of mitochondrial function can also result in cell cycle disruption. Mitochondrial dynamics can influence G1-S phase transition and imbalances in fusion and fission have been shown to drive lung cancer cell proliferation.[62,63] Damage to mtDNA has been shown to activate the cell cycle regulatory kinase, Chk-2, trigger S-phase arrest, and cause a secondary block in G2/M phase.[13] In synchronized cells populations, $\Delta\psi_{mt}$ increased with progression through G2/M phase.[14] Conversely, loss of $\Delta\psi_{mt}$ causes a G2/M block. MIA PaCa-2 cells treated with Mito-Chlor exhibited a cell cycle profile that was consistent with a mechanism of action that involved mtDNA damage at an earlier time point, followed by a decline in $\Delta\psi_{mt}$. Similar to the chlorambucil treated cells, the percentage of hypo-diploid cells observed at the end of 72 h was in accord with the IC_{50} concentration. Given that changes in cell cycle distribution are related to the mechanism of action for a compound or drug, these results indicate that altering subcellular localization can influence mechanism of action.

Despite its mitochondrial localization, Mito-Chlor promoted nDNA damage, as indicated by the time and dose dependent increase in histone H2A.X phosphorylation. On the basis of the reversibility observed in the presence of *N*-acetyl cysteine, we concluded that nDNA damage would be the result of oxidative stress. Several possible explanations for increased ROS production by mitochondria in response to Mito-Chlor are feasible. ROS production may be related to the presence of the phosphonium cation: novel phosphonium salts discovered in our laboratory have been shown to cause rapid and sustained increases in mitochondrial superoxide and cytosolic hydrogen peroxide levels along with increased γH2A.X expression.[50,64] It is also possible that mtDNA damage itself may be the cause of enhanced ROS.[65] In an indirect manner, the loss of oxidative phosphorylation as a result of mtDNA depletion can also increase the formation of oxygen radicals capable of inducing nDNA damage.[65] The increase in γH2A.X expression could be due to incomplete repair of nonlethal, nonpathological levels of ROS as mtDNA depletion can inhibit the repair of oxidative damage in nDNA.[66] It is important to note that the reversal of γH2A.X expression by NAC had no significant impact on the growth inhibitory properties of Mito-Chlor. These results indicate that ROS-induced nDNA damage is secondary to the mechanism of action of Mito-Chlor.

Remarkably, the enhanced drug potency observed in our cell-based assays translated to a robust reduction in tumor volume in vivo. Established tumors treated with Mito-Chlor as a single agent were significantly smaller in size compared to vehicle treated mice. Having delayed tumor growth when administered as a single agent, it is likely that Mito-Chlor could improve treatment responses when added to current pancreatic cancer chemotherapeutic regimens.

In addition to the pharmacological advantages gained, mitochondrial targeting of chlorambucil will be an important tool to study the role of mitochondrial DNA damage in nitrogen mustard-induced cell death. It has long been known that both the nuclear and mitochondrial genomes are targets of nitrogen mustards, but the contribution of mtDNA damage in promoting cell death remained unclear due to an inability to selectively promote damage within this cell compartment. To this end, our study provides strong evidence that mtDNA damage is sufficient to cause cell death and that this cell death occurs by a mechanism distinct from that occurring with nontargeted chlorambucil.

■ CONCLUSIONS

Nitrogen mustards, such as chlorambucil, have a long history of safety and efficacy in chemotherapeutic regimens but drug resistance and risk of secondary neoplasms remain serious sequelae. We designed a triphenylphosphonium derivative of chlorambucil, Mito-Chlor, that targets cancer cell mitochondria based on altered mitochondrial membrane potential $\Delta\psi_{mt}$. We have shown that this type of targeting has reversed drug resistance in panels of breast and pancreatic cancer cell lines. Preliminary mechanistic studies demonstrate Mito-Chlor's mechanism of action to be distinct from that of chlorambucil. Taken together, these results provide the basis for further preclinical evaluation as potential therapeutic for treatment refractory breast and pancreatic tumors. In addition to its clinical benefits, Mito-Chlor is also a valuable tool to study nitrogen mustard induced mtDNA damage.

■ EXPERIMENTAL SECTION

Materials. Chlorambucil was purchased from Oakwood Products, Inc., and antitriphenylphosphonium antisera was a gift from Dr. Mike Murphy (Medical Research Council, Cambridge, UK).

Cell Culture. The cell lines used were purchased from the American Type Culture Collection (ATCC) with the exception of the MDA-MB-231 Rho θ and MDA-MB-435 Rho θ cell lines, which were generated in-house using the method described by Hashigushi.[67] Cell lines were maintained in the appropriate growth media (DMEM for MDA-MB-435, MDA-MB-435 Rho θ, MDA-MB-468, BT549, MCF7, SKBR3, and MIAPaCa-2 cell lines, and RPMI for the BxPC3, MDA-MB-231, MDA-MB-231 Rho θ, Hs578T, and CAMA-1 cell lines) supplemented with 10% fetal bovine serum and 2 mM L-gutamine at 37 °C in a humidified atmosphere of 5% CO_2. MDA-MB-435 Rho θ and MDA-MB-231 Rho θ cell lines were additionally supplemented with 50 μg/mL uridine. All experiments were performed in a growth media using subconfluent cells in the exponential growth phase. For use in tissue culture experiments, chlorambucil and Mito-Chlor were prepared at 100 and 10 mM concentrations, respectively, in sterile dimethylsulfoxide (DMSO) and stored at −20 °C as single-use aliquots.

Analysis of DNA Content by Flow Cytometry. MIA PaCa-2 were grown in 6 well culture dishes were treated with IC_{50} concentrations of chlorambucil and Mito-Chlor. At the indicated time points, cells were harvested with trypsin and washed with 1× PBS prior to fixation and permeabilization with 70% ethanol. Fixed cells were stained in a 10 μg/mL solution of propidium iodide containing 100 μg/mL RNase A prior to analysis for DNA content. Sample readings were performed using a BD-LSR II flow cytometer equipped with a 488 nm diode-pulse solid state laser and 550 nm dichroic mirror and 575/26 nm bandpass filter.

MTT Assay. Cytotoxicity was assessed by 3-(4,5-dimethylthiazol-2-yl)-2,5-diphenyltetrazolium bromide (MTT) assay. Briefly, cells were seeded in 96-well tissue culture dishes at a density of 4×10^3 cells per well and allowed to adhere overnight. Cells were subsequently continuously treated with drugs for 72 h. Media was refreshed, and an MTT solution was then added to each well to give a final concentration of 0.3 mg/mL MTT. Cells were incubated with MTT for 4 h at 37 °C. After removal of the supernatant, DMSO was added and the amount of insoluble purple formazan was measured spectrophotometrically at λ_{max}= 570 nm. All assays were done in triplicate. The IC_{50} was calculated for each treatment from a plot of log drug concentration versus percentage of nonviable cells.

Confocal Microscopy of Fixed Cells. For determination of the subcellular localization of Mito-Chlor, MIA PaCa-2 cells were seeded on glass coverslips at a density of 50000 cells and allowed to adhere overnight. The following day, MIA PaCa-2 cells were treated with 100 μM chlorambucil or 10 μM Mito-Chlor for 18 h. At the end of treatment, media was removed and cells were washed with 500 μL of 1× PBS prior to fixation with 3.7% formaldehyde for 15 min at room temperature. Fixed cells were washed with 500 μL of 1× PBS prior and subsequent to permeabilization with ice-cold acetone for 5 min at −20 °C. Coverslips were blocked for 30 m with 1% bovine serum albumin (BSA) in PBS to inhibit nonspecific antibody binding prior to incubation overnight at 4 °C with immuno-capture antibody raised against complex I or antisera recognizing the triphenylphosphonium moiety, each diluted 1:1000 in 1% BSA/PBS. Antibodies were removed, and coverslips were washed 500 μL of 1× PBS with gentle agitation. Goat-antirabbit Cy5-conjugated and goat-antimouse Cy3-conjugated antibodies were diluted 1:200 in 1% BSA/PBS and incubated with coverslips for 2 h. Coverslips were again washed with 1× PBS under gentle agitation, air-dried, and mounted on precleaned glass slides using Prolong Gold antifade mounting media. Images were obtained using a Leica SP2 scanning confocal microscope equipped with 488 nm argon and 633 nM krypton lasers and Leica Confocal Software v. 2.61.

SDS-PAGE and Western Blotting. For these studies whole cell lysates were prepared from MIA PaCa-2 and MDA-MB-468 cells treated for varying durations of time with their respective IC_{50} concentrations of chlorambucil or Mito-Chlor in the presence or the absence of 10 mM *N*-acetylcysteine. To this end, cell monolayers were washed with 1× PBS and scraped into ice-cold RIPA buffer [50 mM Tris HCl pH 8.0, 150 mM sodium chloride, 1% Nonidet P-40, 0.5% sodium deoxycholate, 0.1% sodium dodecyl sulfate] containing 1× Sigmafast protease inhibitor cocktail. The lysates were cleared by centrifugation at 14000 rpm for 10 min at 4 °C. For SDS-PAGE, 25 μg of protein prepared in SDS loading buffer containing 10 mM DTT was loaded onto a 15% polyacrylamide gel and resolved by electrophoresis for 2 h at 100 V. Proteins were transferred to PVDF membrane. Following electrophoretic transfer, membranes were blocked 1 h with 5% nonfat dry milk prepared in Tris-buffered saline/0.1% Tween-20 (NFDM/TBST). Primary antibodies were prepared in either 5% bovine serum albumin (BSA/TBST) or 5% NFDM/TBST according to the manufacturer's guidelines. Secondary antibodies were prepared in NFDM/TBST. Blots were incubated with primary antibodies (1:1000 dilution) overnight at 4 °C and with horseradish peroxidase-conjugated (HRP) secondary antibodies (1:5000) for 2−4 h at RT. Membranes were washed 3 times for 5 min with TBST following both primary and secondary antibody incubations. HRP-catalyzed chemiluminescence was generated using Durawest supersignal enhanced chemiluminescence substrate. Signals corresponding to levels of protein expression were visualized using Bio.Rad Chemidoc XRS + CCD camera and Quantity One detection software.

In Vivo Studies. Mouse xenograft studies were performed in 4−6 week old athymic nude mice. To establish xenografts, 2×10^6 MIA PaCa-2 cells prepared in a 1:1 suspension of matrigel−basal DMEM were injected subcutaneously into the right rear flank of anesthetized mice. Once tumors became palpable, measurements in two dimensions were obtained using Vernier calipers. Tumor volume was calculated based on the equation:

$$V = d^2 \times D/2$$

where d represents the smaller of the two dimensions and D represents the larger dimension. When tumor volumes reached approximately 100 mm^3, mice were randomized to treatment groups (n = 6 mice per treatment group). Initially, treatments were prepared as a suspension in normal saline/0.5% Solutol HS 15. Due to adverse events attributable to the surfactant properties of the solubilizing agent, the formulations were modified. Chlorambucil was prepared as a 20× stock in DMSO and diluted in saline. Mito-Chlor stock was prepared at a similar concentration and diluted in pure sesame oil. Throughout the course of the experiment, treatments were administered via an intraperitoneal (ip) injection at doses of 10 mg/kg of body weight, five times weekly. Dosing was chosen based on a survey of literature involving the use of chlorambucil in mouse models, with the dose 10 mg/kg being shown to have the greatest efficacy with the fewest side effects. For comparison, Mito-Chlor was dosed at the same concentration as the parent drug. Health checks were performed on a daily basis. Acute toxicity and tumor volume >1600 mm^3 were regarded as terminal end points requiring removal mice from the study. Upon cessation of treatment, mice were euthanized and necropsied. Tumor and organ samples were harvested at the time of euthanasia and processed as frozen and formalin-fixed samples. All procedures were carried out in accordance with the IACUC protocols at the University of Southern California. Statistical analysis was performed using an unpaired Student's t-test.

JC-1 Staining for $\Delta\psi_{mt}$. MDA-MB-231 Rho wild-type and MDA-MB-231 Rho θ cells were trypsinized and collected by centrifugation at 1200 rpm for 5 min at RT. Cell pellets were washed with 1× PBS, centrifuged, and resuspended in basal media containing 10 μg/mL JC-1 dye. Cells were incubated for 15 min in a 37 °C water bath. In preparation for the analysis, cells were centrifuged at 5000 rpm for 5 min at room temperature in a microcentrifuge. Pelleted cells were resuspended in 1× PBS and kept on ice. Mitochondrial membrane potential was determined as the ratio of mean red fluorescence intensity to green fluorescence intensity. Mean fluorescence intensity was measured on a BD LSRII flow cytometer using detectors equipped to capture light emitted in the 525−590 nm range following an excitation at λ_{ex} = 488 nm.

■ ASSOCIATED CONTENT

Ⓢ Supporting Information

Synthesis and characterization of compounds **1**−**5**, figures and tables. This material is available free of charge via the Internet at http://pubs.acs.org.

■ AUTHOR INFORMATION

Corresponding Authors

*For B.Z.O.: E-mail, bogdan@usc.edu.

*For N.N.: phone, 734-647-2732; E-mail, neamati@umich.edu. Address: Department of Medicinal Chemistry, College of Pharmacy, University of Michigan, North Campus Research Complex, 2800 Plymouth Road, Building 520, Room 1363, Ann Arbor, Michigan 48109-2800, United States.

Notes

The authors declare no competing financial interest.

■ ACKNOWLEDGMENTS

The work in N.N.'s laboratory was supported in part by Sharon and William Cockrell Endowed Cancer Research Fund and in the laboratory of B.Z.O. in part by the Daniel Tsai Fund for Translational Research. J.D.G. thanks the American Foundation for Pharmaceutical Education (AFPE) and USC School of Pharmacy for fellowship support.

■ ABBREVIATIONS USED

TPP, triphenylphosphonium; mtDNA, mitochondrial DNA; nDNA, nuclear DNA; ROS, reactive oxygen species; CLL, chronic lymphocytic leukemia; DSB, double-strand breaks; NER, nucleotide excision repair; HR, homologous recombination; NHEJ, nonhomologous end joining; BRCA1, breast cancer 1, early onset; NAC, *N*-acetyl-cysteine; $\Delta\psi_{mt}$, mitochondrial membrane potential; PAAM, phenyl acetic acid mustard; γH2A.X, phosphorylated histone H2A.X; BRCA2 breast cancer 2, early onset; FANCC, Fanconi anemia, complementation group C; FANCG, Fanconi anemia, complementation group G; PARP, poly(adenosine diphosphate-ribose) polymerase; ROS, reactive oxygen species

■ REFERENCES

(1) Chabner, B. A.; Bertino, J.; Cleary, J.; Ortiz, T.; Lane, A.; Supko, J. G.;;Ryan, D. Cytotoxic Agents. In *Goodman & Gilman's Pharmacologic Basis of Therapeutics*:, 12th ed.; Brunton, L. L., C., B., Knollmann, B. C., Ed.; McGraw-Hill: New York, 2011; Chapter 61.

(2) Kohn, K. W. *Molecular Aspects of Anti-Cancer Drug Action*; Macmillan Publishers: London, 1980; pp 233−282.

(3) Kohn, K. W.; Hartley, J. A.; Mattes, W. B. Mechanisms of DNA sequence selective alkylation of guanine-N7 positions by nitrogen mustards. *Nucleic Acids Res.* **1987**, *15*, 10531−10549.

(4) Hemminki, K.; Ludlum, D. B. Covalent modification of DNA by antineoplastic agents. *J. Natl. Cancer Inst.* **1984**, *73*, 1021−1028.

(5) Hansson, J.; Lewensohn, R.; Ringborg, U.; Nilsson, B. Formation and removal of DNA cross-links induced by melphalan and nitrogen mustard in relation to drug-induced cytotoxicity in human melanoma cells. *Cancer Res.* **1987**, *47*, 2631−2637.

(6) Panasci, L.; Paiement, J.-P.; Christodoulopoulos, G.; Belenkov, A.; Malapetsa, A.; Aloyz, R. Chlorambucil drug resistance in chronic lymphocytic leukemia. *Clin. Cancer Res.* **2001**, *7*, 454−461.

(7) Catovsky, D.; Else, M.; Richards, S. Chlorambucil—still not bad: a reappraisal. *Clin. Lymphoma Myeloma* **2011**, *11* (Leuk. Suppl 1), S2−S6.

(8) Knauf, W. U.; Lissitchkov, T.; Aldaoud, A.; Liberati, A. M.; Loscertales, J.; Herbrecht, R.; Juliusson, G.; Postner, G.; Gercheva, L.; Goranov, S.; Becker, M.; Fricke, H. J.; Huguet, F.; Del Giudice, I.; Klein, P.; Merkle, K.; Montillo, M. Bendamustine compared with chlorambucil in previously untreated patients with chronic lymphocytic leukaemia: updated results of a randomized phase III trial. *Br. J. Hamaetol.* **2012**, *159*, 67−77.

(9) Chen, L. B. Mitochondrial membrane potential in living cells. *Annu. Rev. Cell Biol.* **1988**, *4*, 155−181.

(10) Cullinane, C.; Bohr, V. A. DNA interstrand cross-links induced by psoralen are not repaired in mammalian mitochondria. *Cancer Res.* **1998**, *58*, 1400−1404.

(11) LeDoux, S. P.; Wilson, G. L.; Beecham, E. J.; Stevnsner, T.; Wassermann, K.; Bohr, V. A. Repair of mitochondrial DNA after various types of DNA damage in Chinese hamster ovary cells. *Carcinogenesis* **1992**, *13*, 1967−1973.

(12) Amrein, L.; Loignon, M.; Goulet, A. C.; Dunn, M.; Jean-Claude, B.; Aloyz, R.; Panasci, L. Chlorambucil cytotoxicity in malignant B lymphocytes is synergistically increased by 2-(morpholin-4-yl)-benzo-[*h*]chomen-4-one (NU7026)-mediated inhibition of DNA double-strand break repair via inhibition of DNA-dependent protein kinase. *J. Pharmacol. Exp. Ther.* **2007**, *321*, 848−855.

(13) Koczor, C. A.; Shokolenko, I. N.; Boyd, A. K.; Balk, S. P.; Wilson, G. L.; LeDoux, S. P. Mitochondrial DNA damage initiates a cell cycle arrest by a Chk2-associated mechanism in mammalian cells. *J. Biol. Chem.* **2009**, *284*, 36191−36201.

(14) Martinez-Diez, M.; Santamaria, G.; Ortega, Å. D.; Cuezva, J. M. Biogenesis and dynamics of mitochondria during the cell cycle: significance of 3′UTRs. *PLoS One* **2006**, *1*, e107.

(15) Kuo, L. J.; Yang, L. X. g-H2AX—a novel biomarker for DNA double-strand breaks. *In Vivo* **2008**, *22*, 305−309.

(16) Pedersen, P. J.; Christensen, M. S.; Ruysschaert, T.; Linderoth, L.; Andresen, T. L.; Melander, F.; Mouritsen, O. G.; Madsen, R.; Clausen, M. H. Synthesis and biophysical characterization of chlorambucil anticancer ether lipid prodrugs. *J. Med. Chem.* **2009**, *52*, 3408−3415.

(17) Myrberg, H.; Zhang, L.; Mae, M.; Langel, U. Design of a tumor-homing cell-penetrating peptide. *Bioconjugate Chem.* **2008**, *19*, 70−75.

(18) Bielawski, K.; Bielawska, A. Small-molecule based delivery systems for alkylating antineoplastic compounds. *ChemMedChem* **2008**, *3*, 536−542.

(19) Beyer, U.; Roth, T.; Schumacher, P.; Maier, G.; Unold, A.; Frahm, A. W.; Fiebig, H. H.; Unger, C.; Kratz, F. Synthesis and in vitro efficacy of transferrin conjugates of the anticancer drug chlorambucil. *J. Med. Chem.* **1998**, *41*, 2701−2708.

(20) Stark, P. A.; Thrall, B. D.; Meadows, G. G.; Abdel-Monem, M. M. Synthesis and evaluation of novel spermidine derivatives as targeted cancer chemotherapeutic agents. *J. Med. Chem.* **1992**, *35*, 4264−4269.

(21) Descoteaux, C.; Brasseur, K.; Leblanc, V.; Parent, S.; Asselin, E.; Berube, G. Design of novel tyrosine−nitrogen mustard hybrid molecules active against uterine, ovarian and breast cancer cell lines. *Steroids* **2012**, *77*, 403−412.

(22) Guaragna, A.; Chiaviello, A.; Paolella, C.; D'Alonzo, D.; Palumbo, G. Synthesis and evaluation of folate-based chlorambucil delivery systems for tumor-targeted chemotherapy. *Bioconjugate Chem.* **2012**, *23*, 84−96.

(23) Bielawska, A.; Bielawski, K.; Muszynska, A. Synthesis and biological evaluation of new cyclic amidine analogs of chlorambucil. *Farmaco* **2004**, *59*, 111−117.

(24) Clavel, C. M.; Zava, O.; Schmitt, F.; Kenzaoui, B. H.; Nazarov, A. A.; Juillerat-Jeanneret, L.; Dyson, P. J. Thermoresponsive chlorambucil derivatives for tumour targeting. *Angew. Chem., Int. Ed. Engl.* **2011**, *50*, 7124−7127.

(25) Goff, R. D.; Thorson, J. S. Assessment of chemoselective neoglycosylation methods using chlorambucil as a model. *J. Med. Chem.* **2010**, *53*, 8129−8139.

(26) Descoteaux, C.; Leblanc, V.; Brasseur, K.; Gupta, A.; Asselin, E.; Berube, G. Synthesis of D- and L-tyrosine-chlorambucil analogs active against breast cancer cell lines. *Bioorg. Med. Chem. Lett.* **2010**, *20*, 7388−7392.

(27) Gupta, A.; Saha, P.; Descoteaux, C.; Leblanc, V.; Asselin, E.; Berube, G. Design, synthesis and biological evaluation of estradiol−chlorambucil hybrids as anticancer agents. *Bioorg. Med. Chem. Lett.* **2010**, *20*, 1614−1618.

(28) Evers, B.; Schut, E.; van der Burg, E.; Braumuller, T. M.; Egan, D. A.; Holstege, H.; Edser, P.; Adams, D. J.; Wade-Martins, R.; Bouwman, P.; Jonkers, J. A high-throughput pharmaceutical screen identifies compounds with specific toxicity against BRCA2-deficient tumors. *Clin. Cancer Res.* **2010**, *16*, 99−108.

(29) van der Heijden, M. S.; Brody, J. R.; Dezentje, D. A.; Gallmeier, E.; Cunningham, S. C.; Swartz, M. J.; DeMarzo, A. M.; Offerhaus, G. J.; Isacoff, W. H.; Hruban, R. H.; Kern, S. E. In vivo therapeutic responses contingent on Fanconi anemia/BRCA2 status of the tumor. *Clin. Cancer Res.* **2005**, *11*, 7508−7515.

(30) Heerdt, B. G.; Houston, M. A.; Augenlicht, L. H. Growth properties of colonic tumor cells are a function of the intrinsic mitochondrial membrane potential. *Cancer Res.* **2006**, *66*, 1591−1596.

(31) Heerdt, B. G.; Houston, M. A.; Augenlicht, L. H. The intrinsic mitochondrial membrane potential of colonic carcinoma cells is linked to the probability of tumor progression. *Cancer Res.* **2005**, *65*, 9861−9867.

(32) Heerdt, B. G.; Houston, M. A.; Wilson, A. J.; Augenlicht, L. H. The intrinsic mitochondrial membrane potential ($\Delta\psi$m) is associated with steady-state mitochondrial activity and the extent to which colonic epithelial cells undergo butyrate-mediated growth arrest and apoptosis. *Cancer Res.* **2003**, *63*, 6311−6319.

(33) Fedeles, B. I.; Zhu, A. Y.; Young, K. S.; Hillier, S. M.; Proffitt, K. D.; Essigmann, J. M.; Croy, R. G. Chemical genetics analysis of an aniline mustard anticancer agent reveals complex I of the electron transport chain as a target. *J. Biol. Chem.* **2011**, *286*, 33910−33920.

(34) Hillier, S. M.; Marquis, J. C.; Zayas, B.; Wishnok, J. S.; Liberman, R. G.; Skipper, P. L.; Tannenbaum, S. R.; Essigmann, J. M.; Croy, R. G. DNA adducts formed by a novel antitumor agent 11beta-dichloro in vitro and in vivo. *Mol. Cancer Ther.* **2006**, *5*, 977−984.
(35) Fonseca, S. B.; Pereira, M. P.; Mourtada, R.; Gronda, M.; Horton, K. L.; Hurren, R.; Minden, M. D.; Schimmer, A. D.; Kelley, S. O. Rerouting chlorambucil to mitochondria combats drug deactivation and resistance in cancer cells. *Chem. Biol.* **2011**, *18*, 445−453.
(36) Agapova, L. S.; Chernyak, B. V.; Domnina, L. V.; Dugina, V. B.; Efimenko, A. Y.; Fetisova, E. K.; Ivanova, O. Y.; Kalinina, N. I.; Khromova, N. V.; Kopnin, B. P.; Kopnin, P. B.; Korotetskaya, M. V.; Lichinitser, M. R.; Lukashev, A. L.; Pletjushkina, O. Y.; Popova, E. N.; Skulachev, M. V.; Shagieva, G. S.; Stepanova, E. V.; Titova, E. V.; Tkachuk, V. A.; Vasiliev, J. M.; Skulachev, V. P. Mitochondria-targeted plastoquinone derivatives as tools to interrupt execution of the aging program. 3. Inhibitory effect of SkQ1 on tumor development from p53-deficient cells. *Biochemistry (Moscow)* **2008**, *73*, 1300−1316.
(37) Ross, M. F.; Da Ros, T.; Blaikie, F. H.; Prime, T. A.; Porteous, C. M.; Severina, I. I.; Skulachev, V. P.; Kjaergaard, H. G.; Smith, R. A.; Murphy, M. P. Accumulation of lipophilic dications by mitochondria and cells. *Biochem. J.* **2006**, *400*, 199−208.
(38) Ross, M. F.; Kelso, G. F.; Blaikie, F. H.; James, A. M.; Cocheme, H. M.; Filipovska, A.; Da Ros, T.; Hurd, T. R.; Smith, R. A.; Murphy, M. P. Lipophilic triphenylphosphonium cations as tools in mitochondrial bioenergetics and free radical biology. *Biochemistry (Moscow)* **2005**, *70*, 222−230.
(39) Liberman, E. A.; Topaly, V. P.; Tsofina, L. M.; Jasaitis, A. A.; Skulachev, V. P. Mechanism of coupling of oxidative phosphorylation and the membrane potential of mitochondria. *Nature* **1969**, *222*, 1076−1078.
(40) Murphy, M. P. Targeting lipophilic cations to mitochondria. *Biochim. Biophys. Acta, Bioenerg.* **2008**, *1777*, 1028−1031.
(41) Ross, M. F.; Prime, T. A.; Abakumova, I.; James, A. M.; Porteous, C. M.; Smith, R. A.; Murphy, M. P. Rapid and extensive uptake and activation of hydrophobic triphenylphosphonium cations within cells. *Biochem. J.* **2008**, *411*, 633−645.
(42) Snow, B. J.; Rolfe, F. L.; Lockhart, M. M.; Frampton, C. M.; O'Sullivan, J. D.; Fung, V.; Smith, R. A.; Murphy, M. P.; Taylor, K. M. A double-blind, placebo-controlled study to assess the mitochondria-targeted antioxidant MitoQ as a disease-modifying therapy in Parkinson's disease. *Movement Disord.* **2010**, *25*, 1670−1674.
(43) Gane, E. J.; Weilert, F.; Orr, D. W.; Keogh, G. F.; Gibson, M.; Lockhart, M. M.; Frampton, C. M.; Taylor, K. M.; Smith, R. A.; Murphy, M. P. The mitochondria-targeted anti-oxidant mitoquinone decreases liver damage in a phase II study of hepatitis C patients. *Liver Int.* **2010**, *30*, 1019−1026.
(44) Smith, R. A. J.; Murphy, M. P. Animal and human studies with the mitochondria-targeted antioxidant MitoQ. *Ann. N. Y. Acad. Sci.* **2010**, *1201*, 96−103.
(45) Zhou, Y.; Liu, S. ^{64}Cu-labeled phosphonium cations as PET radiotracers for tumor imaging. *Bioconjugate Chem.* **2011**, *22*, 1459−1472.
(46) Li, Z.; Lopez, M.; Hardy, M.; McAllister, D. M.; Kalyanaraman, B.; Zhao, M. A (99m)Tc-labeled triphenylphosphonium derivative for the early detection of breast tumors. *Cancer Biother. Radiopharm.* **2009**, *24*, 579−587.
(47) Yang, C. T.; Kim, Y. S.; Wang, J.; Wang, L.; Shi, J.; Li, Z. B.; Chen, X.; Fan, M.; Li, J. J.; Liu, S. ^{64}Cu-labeled 2-(diphenylphosphoryl)ethyldiphenylphosphonium cations as highly selective tumor imaging agents: effects of linkers and chelates on radiotracer biodistribution characteristics. *Bioconjugate Chem.* **2008**, *19*, 2008−2022.
(48) Wang, J.; Yang, C. T.; Kim, Y. S.; Sreerama, S. G.; Cao, Q.; Li, Z. B.; He, Z.; Chen, X.; Liu, S. 64Cu-Labeled triphenylphosphonium and triphenylarsonium cations as highly tumor-selective imaging agents. *J. Med. Chem.* **2007**, *50*, 5057−5069.
(49) Madar, I.; Weiss, L.; Izbicki, G. Preferential accumulation of (3)H-tetraphenylphosphonium in non-small cell lung carcinoma in mice: comparison with (99m)Tc-MIBI. *J. Nucl. Med.* **2002**, *43*, 234−238.
(50) Millard, M.; Pathania, D.; Shabaik, Y.; Taheri, L.; Deng, J.; Neamati, N. Preclinical evaluation of novel triphenylphosphonium salts with broad-spectrum activity. *PLoS One* **2010**, *5*, e13131.
(51) Manetta, A.; Gamboa, G.; Nasseri, A.; Podnos, Y. D.; Emma, D.; Dorion, G.; Rawlings, L.; Carpenter, P. M.; Bustamante, A.; Patel, J.; Rideout, D. Novel phosphonium salts display in vitro and in vivo cytotoxic activity against human ovarian cancer cell lines. *Gynecol. Oncol.* **1996**, *60*, 203−212.
(52) McLean, A.; Newell, D.; Baker, G.; Connors, T. The metabolism of chlorambucil. *Biochem. Pharmacol.* **1980**, *29*, 2039−2047.
(53) Lee, F. Y.; Coe, P.; Workman, P. Pharmacokinetic basis for the comparative antitumour activity and toxicity of chlorambucil, phenylacetic acid mustard and beta, beta-difluorochlorambucil (CB 7103) in mice. *Cancer Chemother. Pharmacol.* **1986**, *17*, 21−9.
(54) Mirkes, P. E.; Greenaway, J. C. Teratogenicity of chlorambucil in rat embryos in vitro. *Teratology* **1982**, *26*, 135−143.
(55) Hidalgo, M. Pancreatic cancer. *N. Engl. J. Med.* **2010**, *362*, 1605−17.
(56) Mathews, L. A.; Cabarcas, S. M.; Hurt, E. M.; Zhang, X.; Jaffee, E. M.; Farrar, W. L. Increased expression of DNA repair genes in invasive human pancreatic cancer cells. *Pancreas* **2011**, *40*, 730−739.
(57) Mao, Z.; Jiang, Y.; Liu, X.; Seluanov, A.; Gorbunova, V. DNA repair by homologous recombination, but not by nonhomologous end joining, is elevated in breast cancer cells. *Neoplasia* **2009**, *11*, 683−691.
(58) Li, Y.-H.; Wang, X.; Pan, Y.; Lee, D.-H.; Chowdhury, D.; Kimmelman, A. C. Inhibition of non-homologous end joining repair impairs pancreatic cancer growth and enhances radiation response. *PLoS One* **2012**, *7*, e39588.
(59) Kondo, N.; Takahashi, A.; Ono, K.; Ohnishi, T. DNA damage induced by alkylating agents and repair pathways. *J. Nucleic Acids* **2010**, *2010*, 543531.
(60) Shaheen, M.; Allen, C.; Nickoloff, J. A.; Hromas, R. Synthetic lethality: exploiting the addiction of cancer to DNA repair. *Blood* **2011**, *117*, 6074−6082.
(61) Mourtada, R.; Fonseca, S. B.; Wisnovsky, S. P.; Pereira, M. P.; Wang, X.; Hurren, R.; Parfitt, J.; Larsen, L.; Smith, R. A.; Murphy, M. P.; Schimmer, A. D.; Kelley, S. O. Redirecting an alkylating agent to mitochondria alters drug target and cell death mechanism. *PLoS One* **2013**, *8*, e60253.
(62) Owusu-Ansah, E.; Yavari, A.; Mandal, S.; Banerjee, U. Distinct mitochondrial retrograde signals control the G1-S cell cycle checkpoint. *Nature Genet.* **2008**, *40*, 356−361.
(63) Rehman, J.; Zhang, H. J.; Toth, P. T.; Zhang, Y.; Marsboom, G.; Hong, Z.; Salgia, R.; Husain, A. N.; Wietholt, C.; Archer, S. L. Inhibition of mitochondrial fission prevents cell cycle progression in lung cancer. *FASEB J* **2012**, *26*, 2175−2186.
(64) Shabaik, Y. H.; Millard, M.; Neamati, N. Mechanistic evaluation of a novel small molecule targeting mitochondria in pancreatic cancer cells. *PLoS One* **2013**, *8*, e54346.
(65) Tann, A. W.; Boldogh, I.; Meiss, G.; Qian, W.; Van Houten, B.; Mitra, S.; Szczesny, B. Apoptosis induced by persistent single-strand breaks in the mitochondrial genome: critical role of EXOG (5′EXO/endonuclease) in their repair. *J. Biol. Chem.* **2011**, *286*, 31975−31983.
(66) Delsite, R. L.; Rasmussen, L. J.; Rasmussen, A. K.; Kalen, A.; Goswami, P. C.; Singh, K. K. Mitochondrial impairment is accompanied by impaired oxidative DNA repair in the nucleus. *Mutagenesis* **2003**, *18*, 497−503.
(67) Hashiguchi, K.; Zhang-Akiyama, Q.-M. Establishment of human cell lines lacking mitochondrial DNA. In *Mitochondrial DNA*; Stuart, J. A., Ed.; Humana Press: Totowa, NJ, 2009; Vol. *554*, pp 383−391.